Gravitational Waves versus Electromagnetic Emission in Gamma-Ray Bursts

Jorge A. Rueda* and Remo Ruffini†
Dipartimento di Fisica and ICRA, Sapienza Università di Roma, P.le Aldo Moro 5, I–00185 Rome, Italy and ICRANet, P.zza della Repubblica 10, I–65122 Pescara, Italy
(Dated: March 6, 2013)

The recent progress in the understanding the physical nature of neutron star equilibrium configurations and the first observational evidence of a genuinely Short Gamma-Ray Burst, GRB 090227B, allows to give an estimate of the gravitational waves versus electromagnetic emission in a Gamma-Ray Burst.

We first recall that we have recently proved [1–3] how the consistent treatment of neutron star equilibrium configurations, taking into account the strong, weak, electromagnetic, and gravitational interactions, implies the solution of the general relativistic Thomas-Fermi equations, coupled with the Einstein-Maxwell system of equations. This new set of equations supersed the traditional Tolman-Oppenheimer-Volkoff (TOV) equations [4, 5], which impose the condition of local charge neutrality throughout the configuration (see e.g. [6] and references therein).

The solution of the Einstein-Maxwell-Thomas-Fermi coupled differential equations leads to a new structure of the star (see [1], for details): the positively charged core at supranuclear densities, $\rho > \rho_{\rm nuc} \sim 2.7 \times 10^{14}$ g cm^{-3}, is surrounded by an electron distribution of thickness $\gtrsim \hbar/(m_e c)$ and, at lower densities $\rho < \rho_{\rm nuc}$, a neutral ordinary crust. The equilibrium condition given by the constancy of the particle Klein potentials leads to a discontinuity in the density at the core-crust transition and, correspondingly, an overcritical electric field $\sim (m_\pi/m_e)^2 E_c$, where $E_c = m_e^2 c^3/(e\hbar) \sim 1.3 \times 10^{16}$ Volt/cm, develops in the boundary interface; see Fig. 1. In particular, the continuity of the electron Klein potential leads to a decreasing of the electron chemical potential μ_e and density at the core-crust boundary interface. They reach values $\mu_e^{\rm crust} < \mu_e^{\rm core}$ and $\rho_{\rm crust} < \rho_{\rm core}$ at the edge of the crust, where global charge neutrality is achieved (see Fig. 1). We shall adopt some features of these neutron stars computed using the NL3 parameterization [7] of the phenomenological σ-ω-ρ nuclear model [8]; we refer to [1] for details.

For each central density there exists an entire family of core-crust interface boundaries and, correspondingly, a family of crusts with different mass $M_{\rm crust}$ and thickness $\Delta R_{\rm crust}$. The larger $\rho_{\rm crust}$, the smaller the thickness of the core-crust interface, the peak of the electric field, and the larger the $M_{\rm crust}$ and $\Delta R_{\rm crust}$. The configuration with $\rho_{\rm crust} = \rho_{\rm drip} \sim 4.3 \times 10^{11}$ g/cm^3 separates neutron stars with and without inner crust. All the above new features lead to crusts with masses and thickness smaller than the ones obtained from the traditional TOV treatment. The mass-radius relation obtained in this case have been compared and contrasted with the one obtained from the locally neutral TOV approach; see Fig. 2 and [1] for details.

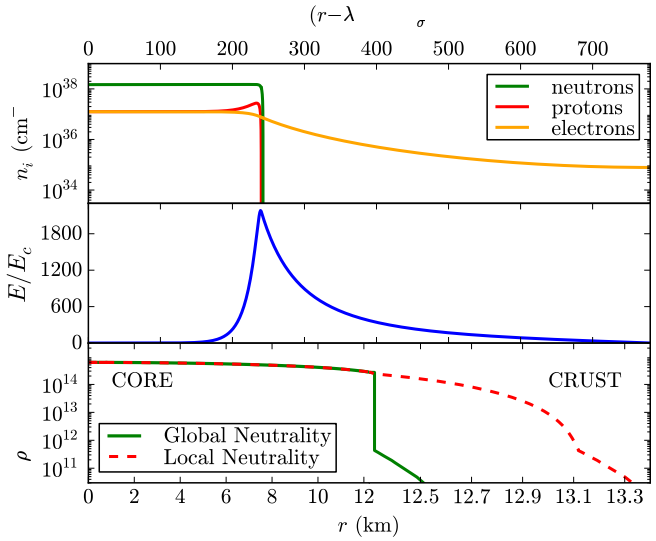

FIG. 1: Upper panel: particle density profiles in the core-crust boundary interface, in units of cm^{-3}. Middle panel: electric field in the core-crust transition layer, in units of the critical field E_c. Lower panel: density profile inside a neutron star with central density $\rho(0) \sim 5\rho_{\rm nuc}$. We compare and contrast the structural differences between the solution obtained from the traditional TOV equations (locally neutral case) and the globally neutral solution presented in [1]. In this example the density at the edge of the crust is $\rho_{\rm crust} = \rho_{\rm drip} = 4.3 \times 10^{11}$ g/cm^3 and $\lambda_\sigma = \hbar/(m_\sigma c) \sim 0.4$ fm denotes the σ-meson Compton wavelength.

In Fig. 2 we show how our new neutron star theory is in agreement with the most up-to-date stringent observational constraints to the mass-radius relation of neutron stars, that are provided by the largest mass, the largest radius, the highest rotational frequency, and the maximum surface gravity, observed from pulsars [9]. They are imposed by the mass of PSR J1614-2230 $M = 1.97 \pm 0.04 M_\odot$ [10], the lower limit to the radius of RX J1856-3754 [12] (dotted-dashed curve), the 716 Hz PSR J1748-2246ad [15] (dashed curve), and the surface gravity of the neutron star in the Low Mass X-Ray Binary X7 from which 90% confidence level contours of constant R_∞ can be extracted [13] (dotted curves); see

[1] for further details.

The above constraints strongly favor stiff nuclear equations of state such as the ones obtained from relativistic mean field models, which provide high maximum masses for neutron stars [9]. In addition, the radius of a canonical neutron star of mass $M = 1.4M_\odot$ is highly constrained to the range $R \gtrsim 12$ km, ruling out a strange quark hypothesis for these objects. Our new neutron star mass-radius relation fully agrees with all the above requirements, for instance, we find that a canonical neutron star with $M = 1.40M_\odot$ has a radius $R = 12.31$ km, for the NL3 parameterization of the nuclear EoS (see [1], for details).

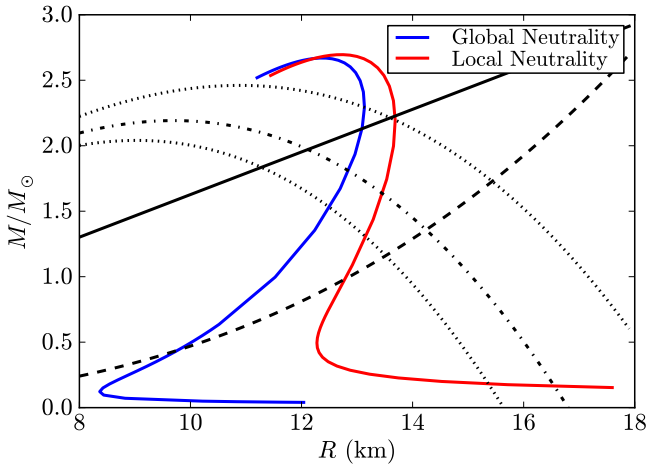

FIG. 2: Constraints on the neutron star mass-radius relation (see [9] and references therein). We compare and contrast the theoretical M-R relation of globally neutral neutron stars [1] (blue curve) obtained from the solution of the Einstein-Maxwell-Thomas-Fermi equations and locally neutral neutron stars (red curve) obtained by solving the TOV equations. Any mass-radius relation have a maximum mass larger than $M = 1.97 \pm 0.04 M_\odot$ and should pass through the area delimited by the solid, dotted-dashed, dashed, and dotted curves.

We now turn to the observations of GRB 090227B (see [16] for details). The progress obtained from the Fermi-GBM and Konus-Wind satellites has been used to identify the new class of genuinely short GRBs: short bursts with the same inner engine of the long GRBs but endowed with a severely low value of the baryon load, $B \equiv M_B c^2/E_{tot}^{GRB} \lesssim 5 \times 10^{-5}$, where M_B is the mass of the baryons engulfed by the expanding ultrarelativistic e^+e^- plasma of energy E_{tot}^{GRB}. The emission from these GRBs mainly consists in a first emission, the peak GRB (P-GRB), followed by a softer emission squeezed on the first one. The typical separation between the two components is expected to be shorter than 1–10 ms.

A special case is GRB 090227B. From the 16 ms time-binned light curves a significant thermal emission in the first 96 ms, which has been identified with the P-GRB, has been found [16]. The subsequent emission is identified with the extended afterglow. The P-GRB of 090227B has the highest temperature ever observed, $k_B T = 517$ keV, where k_B is the Boltzmann constant. The results of the fit of the light curve and spectrum of GRB 090227B are summarized in Table I. In particular we show the total energy emitted E_{tot}^{GRB}, Baryon load B, Lorentz factor at transparency Γ_{tr}, cosmological redshift z, intrinsic duration of the GRB emission Δt, and average density of the CircumBurst Medium (CBM) $\langle n_{CBM} \rangle$; we refer to [16] for further details.

E_{tot}^{GRB} (erg)	2.83×10^{53}
B	4.13×10^{-5}
Γ_{tr}	1.44×10^4
z	1.61
Δt (s)	0.35
$\langle n_{CBM} \rangle$ (cm^{-3})	1.9×10^{-5}

TABLE I: Properties of GRB 090227B: E_{tot}^{GRB} is the total energy emitted in the GRB, B is the Baryon load, Γ_{tr} is the Lorentz factor at transparency, the cosmological redshift is denotes by z, the intrinsic duration of the GRB is Δt, and the average density of the CBM is $\langle n_{CBM} \rangle$. We refer to [16] for additional details.

The above quantitative results lead to the conclusion that the progenitor of GRB 090227B is a neutron star binary: (1) the natal kicks velocities imparted to a neutron star binary at birth can be even larger than 200 km s^{-1} [21] and therefore a binary system can runaway to the halo of its host galaxy (see e.g. [22]), clearly pointing to a very low average number density of the CBM (see e.g. [17–20]); (2) the very large total energy, which we can indeed infer in view of the absence of beaming, and the very short time scale of emission point again to a neutron star binary; (3) as we shall show below the very small value of the baryon load is strikingly consistent with two neutron stars having small crusts, in line with the recent neutron star theory [1].

We now infer the binary component parameters. It is clear that the merging of two neutron stars will lead to a GRB if the total mass of the binary satisfies

$$M_1 + M_2 \gtrsim M_{\rm crit} = 2.67 M_\odot \,, \qquad (1)$$

where $M_{\rm crit}$ is the critical mass over which a neutron star undergoes gravitational collapse to a black hole. The numerical value reported in Eq. (1) has been taken from [1].

Assuming for simplicity a binary with twin components $M_1 = M_2 = M$, we obtain masses $M = 1.335 M_\odot$ and correspondingly radii $R_1 = R_2 = 12.24$ km (see Fig. 2 and [1]). The mass of the corresponding crust of each component is $M_{\rm crust} \sim 3.6 \times 10^{-5} M_\odot$ and the thickness of the crust is $\Delta R_{\rm crust} \sim 0.47$ km.

The location of the binary in the very low interstellar density medium of galactic halos makes possible to probe

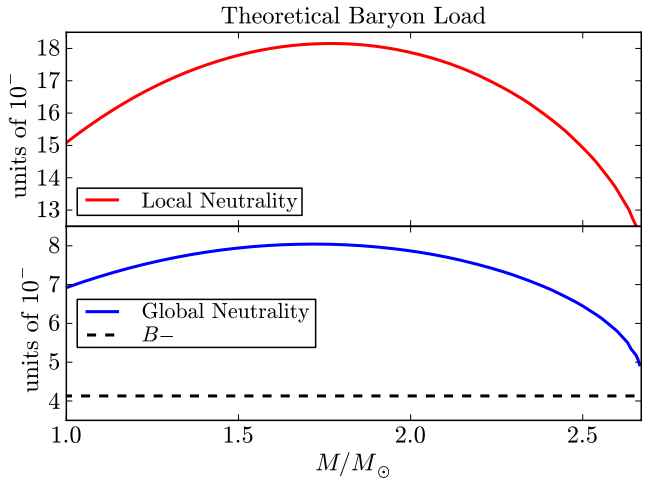

FIG. 3: Baryon load expected to be left by a binary neutron star merger, given by Eq. (2), as a function of the total mass M of globally (lower panel, units 10^{-5}) and locally neutral (upper panel, units 10^{-2}) neutron stars, for the case of GRB 090227B. We have indicated the observed baryon load of GRB 090227B, $B = 4.13 \times 10^{-5}$; see Table I and [16].

the neutron star theory and equation of state through the knowledge of the baryon load B inferred from the fitting of the GRB light curve and spectrum. The baryonic matter which the GRB interact with is in these systems provided by the material of the neutron star crusts ejected during the binary coalescence. Thus, a theoretical expectation of the baryon load B left in a binary neutron star merger is

$$B = \frac{E^B_{\rm crust}}{E^{GRB}_{tot}}\,, \tag{2}$$

where

$$E^B_{\rm crust} \sim \frac{2GM_{\rm core}M_{\rm crust}}{R_{\rm core}}\,, \tag{3}$$

is the mass-energy of the crust material that will be potentially ejected; the factor 2 comes from the fact that both neutron star components contribute to the baryon load.

In Fig. 3 we have plotted the theoretical baryon load given by Eq. (2) for GRB 090227B, namely using $E^{GRB}_{tot} = 2.83 \times 10^{53}$ erg, as a function of the mass M of the globally and locally neutral neutron stars shown in Fig. 2.

The agreement of the observed baryon load of GRB 090227B (see Table I and [16]) with the low mass of the crust obtained from the globally neutral neutron stars of [1] is evident (see Fig. 3). It can be compared and contrasted with the ones obtained enforcing the local charge neutrality condition. For the specific binary neutron star system studied here we obtain a theoretical prediction of the baryon load from Eq. (2), $B \sim E^B_{\rm crust}/E^{GRB}_{tot} \sim 7.6 \times 10^{-5}$, or a mass of the baryons $M_B = E^B_{\rm crust}/c^2 \sim 1.2 \times 10^{-5} M_\odot$, to be confronted with the one obtained from the fitting procedure of GRB 090227B, $B \sim 4.13 \times 10^{-5}$, corresponding to $M_B = BE^{GRB}_{tot}/c^2 \sim 0.7 \times 10^{-5} M_\odot$. The above theoretical predictions of the neutron star crust mass $M_{\rm crust}$ and consequently the value of $E^B_{\rm crust}$ and B have been inferred for a crust with a density at its edge equal to the neutron drip density $\rho_{\rm drip} \sim 4.3 \times 10^{11}$ g cm^{-3}. Neutron star crusts with densities $\rho < \rho_{\rm drip}$ are predicted by the new neutron star theory [1], there is still room for smaller values of the baryonic matter ejected in a binary process, and consequently to still shorter genuinely short GRBs.

The mass-energy of the baryon ejecta obtained from the estimate (2) gives for locally neutral neutron stars values 10^2–10^3 bigger than the ones analyzed before (see Fig. 3), due to the more massive crusts obtained from the TOV-like treatment (see [1] for details). It implies that Eq. (2) gives in such a case $M_B \sim 10^{-3}$–$10^{-2} M_\odot$, in line with previous results obtained from the numerical simulation of the dynamical evolution of neutron star binaries (see e.g. [23, 24]), where locally neutral neutron stars are employed.

We are considering a neutron star binary with components (M_1, R_1) and (M_2, R_2) orbiting each other in a circular orbit of radius a (separation between the two neutron star centers), orbital angular velocity

$$\omega = \sqrt{\frac{G(M_1 + M_2)}{a^3}}\,, \tag{4}$$

and total energy

$$E = -\frac{1}{2}\frac{GM_1M_2}{a}\,. \tag{5}$$

The leading term driving the loss of energy via gravitational wave emission is given by

$$-\frac{dE}{dt} = \frac{32}{5}\frac{G^4}{c^5}\frac{(M_1 + M_2)(M_1M_2)^2}{a^5}\,, \tag{6}$$

which leads to a decreasing of the separation a with time and consequently a shortening of the orbital period $P = 2\pi/\omega$ dictated by $P^{-1}dP/dt = (3/2)a^{-1}da/dt = -(3/2)E^{-1}dE/dt$ [25]. Additional contributions to the gravitational wave power due to higher multipole moments of the components such as angular momentum J and quadrupole moment Q (deformation) are conceptually relevant corrections to the above formula (see e.g. [26] and references therein, for details) although quantitatively negligible. For instance, the first correction due to the spin angular momentum J of the neutron star components is given by $-11/4\, j\omega M$ in geometric units, where $j = cJ/(GM^2)$ is the dimensionless angular momentum parameter. This correction is only of order 10^{-2} for a binary orbit of very high angular frequency $\sim$ kHz and for neutron stars with $M = 1.335 M_\odot$ and

$j = 0.4$. We recall that the fastest observed pulsar, PSR J1748-2246ad, has a rotation frequency of 716 Hz [15], which gives $j \sim 0.51\, I_{45}/(M_0/M_\odot)^2 = 0.26\, I_{45}$ with the latter value for a canonical NS of $M = 1.4 M_\odot$, I_{45} is the moment of inertia in units of 10^{45} g cm^2. The first correction due to the quadrupole deformation multipole moment Q of the neutron star, given by $-2\, Q \omega^{4/3} M^{-5/3}$, is of order 10^{-3} for the same parameters with $Q \sim 4 \times 10^{43}$ g cm$^2 \sim 3$ km^3, the latter value in geometric units.

The gravitational waves emission dominates the energy loss during the spiraling phase while the electromagnetic radiation dominates from the coalescence with the final emission of a short GRB if the total mass of the binary exceeds the critical mass for neutron star gravitational collapse $\sim 2.67 M_\odot$, see Eq. (1). Thus, an upper limit for the gravitational wave emission radiated away can be obtained from the energy difference between the initial binary at time $t_0 = 0$ with separation a_0 and energy E_0, and the binary at time t_f and separation $a_f = R_1 + R_2$, with energy E_f, when the two components *touch* each other. An absolute upper limit for the gravitational wave energy emission, $\Delta E_{GW}^{\rm max}$, can be therefore determined by the assumption of an infinite initial separation $a_0 \to \infty$, i.e.

$$\Delta E_{GW}^{\rm max} = E(t_f) - E(t_0) = \frac{1}{2} \frac{G M_1 M_2}{R_1 + R_2} \,. \qquad (7)$$

For the neutron star binary discussed in this work for GRB 090227B, we obtain the absolute upper bound

$$\Delta E_{GW}^{\rm max} = \frac{1}{4} \frac{G M^2}{R} \sim 9.6 \times 10^{52} \text{ erg} = 0.054 M_\odot c^2 \,, \quad (8)$$

which in the case of the genuinely short GRB 090227B is one order of magnitude smaller than the emitted electromagnetic energy $E_{tot}^{GRB} = 2.83 \times 10^{53}$ erg (see Table I and [16]). It is also worth mentioning that indeed this numerical value (8) limits from above the results of full numerical integrations of the gravitational wave radiation emitted in the neutron star binaries during the entire process of spiraling and merging (see e.g. [23]).

We have shown that the observations of the genuinely short GRB 090227B lead to crucial information on the binary neutron star progenitor. The data obtained from the electromagnetic spectrum allows to probe crucial aspects of the correct theory of neutron stars and their equation of state. The baryon load parameter B obtained from the analysis of GRB 090227B, leads to a most remarkable agreement of the baryonic matter expected to be ejected in a neutron star binary merger and validate the choice of the parameters of the binary components, $M_1 = M_2 = 1.34 M_\odot$, and $R_1 = R_2 = 12.24$ km. This represents a test of the actual neutron star parameters described by the recent developed self-consistent theory of neutron stars [1] that takes into account the strong, weak, electromagnetic and gravitational interactions within general relativity. In view of the above limits given in Eq. (8), it is clear that the emission of electromagnetic radiation in a GRB by a binary neutron star system is at least one order of magnitude larger than the gravitational wave emission.

* Electronic address: jorge.rueda@icra.it
† Electronic address: ruffini@icra.it

[1] R. Belvedere, D. Pugliese, Jorge A. Rueda, R. Ruffini and S.-S. Xue, Nucl. Phys. A **883**, 1 (2012).
[2] Jorge A. Rueda, R. Ruffini and S.-S. Xue, Nucl. Phys. A **872**, 286 (2011).
[3] M. Rotondo, Jorge A. Rueda, R. Ruffini and S.-S. Xue, Phys. Lett. B **701**, 667 (2011).
[4] R. C. Tolman, Phys. Rev. **55**, 364 (1939).
[5] J. R. Oppenheimer and G. Volkoff, Phys. Rev. **55**, 374 (1939).
[6] P. Haensel, A. Y. Potekhin, D. G. Yakovlev, *Neutron Stars 1: Equation of State and Structure*, (Springer, New York 2007).
[7] G. A. Lalazissis, J. König, and P. Ring, Phys. Rev. C **55**, 540 (1997).
[8] J. Boguta and A. R. Bodmer, Nucl. Phys. A **292**, 413 (1977).
[9] J. E. Trümper, Prog. Part. Nucl. Phys. **66**, 674 (2011).
[10] P. B. Demorest, T. Pennucci, S. M. Ransom, M. S. E. Roberts and J. W. T. Hessels, Nature **467**, 1081 (2010).
[11] S. Bhattacharyya, T. E. Sthrohmayer, M. C. Miller and C. B. Markwardt, Astroph. J. **619**, 483 (2005).
[12] J. Trümper, V. Burwitz, F. Harberl and V. E. Zavlin, Nucl. Phys. B Proc. Suppl. **132**, 560 (2004).
[13] C. O. Heinke, G. B. Rybicki, R. Narayan and J. E. Grindlay, Astroph. J. **644**, 1090 (2006).
[14] J. M. Lattimer and M. Prakash, Science **304**, 536 (2004).
[15] J. W. T. Hessels, S. M. Ransom, I. H. Stairs, et al., Science **311**, 1901 (2006).
[16] M. Muccino, R. Ruffini, C. L. Bianco, et al., Astroph. J. submitted; arXiv:1205.6600.
[17] M. G. Bernardini, C. L. Bianco, L. Caito, et al. A&A **474**, L13 (2007).
[18] L. Caito, M. G. Bernardini, C. L. Bianco, et al., A&A **498**, 501 (2009).
[19] L. Caito, L. Amati, M. G. Bernardini, et al., A&A **521**, A80 (2010).
[20] G. de Barros, L. Amati, M. G. Bernardini, et al., A&A **529**, A130 (2011).
[21] C. Fryer and V. Kalogera, Astroph. J. **489**, 244 (1997).
[22] L. Z. Kelley, E. Ramirez-Ruiz, M. Zemp, J. Diemand and I. Mandel, Astroph. J. **725**, L91 (2010).
[23] M. Ruffert and H. T. Janka, A&A **380**, 544 (2001).
[24] S. Goriely,A. Bauswein and H. T. Janka, Astroph. J. **738**, L32 (2011).
[25] L. D. Landau and E. M. Lifshitz, *The Classical Theory of Fields* (Oxford: Pergamon Press, 1975).
[26] F. Ryan, Phys. Rev. D **52**, 5707 (1995).